PALEONTOLOGY

Arctic ice and the ecological rise of the dinosaurs

Paul Olsen[1]*, Jingeng Sha[2]*, Yanan Fang[2], Clara Chang[1], Jessica H. Whiteside[3], Sean Kinney[1], Hans-Dieter Sues[4], Dennis Kent[1,5], Morgan Schaller[6], Vivi Vajda[7]

Abstract: Abundant lake ice-rafted debris in Late Triassic and earliest Jurassic strata of the Junggar Basin of northwestern China (paleolatitude ~71°N) indicates that freezing winter temperatures typified the forested Arctic, despite a persistence of extremely high levels of atmospheric P_{CO_2} (partial pressure of CO_2). Phylogenetic bracket analysis shows that non-avian dinosaurs were primitively insulated, enabling them to access rich deciduous and evergreen Arctic vegetation, even under freezing winter conditions. Transient but intense volcanic winters associated with massive eruptions and lowered light levels led to the end-Triassic mass extinction (201.6 Ma) on land, decimating all medium- to large-sized nondinosaurian, noninsulated continental reptiles. In contrast, insulated dinosaurs were already well adapted to cold temperatures, and not only survived but also underwent a rapid adaptive radiation and ecological expansion in the Jurassic, taking over regions formerly dominated by large noninsulated reptiles.

INTRODUCTION

The Late Triassic and earliest Jurassic are characterized as one of the very few times in Earth history in which there is no evidence of polar glacial ice sheets (*1*). Forests were present all the way to the Pangean North Pole and into the southern latitudes as far as land extended. Although there may have been other contributing factors, the leading hypothesis is that Earth was in a "greenhouse" state because of very high atmospheric P_{CO_2} (partial pressure of CO_2) ~1000 to ~6000 parts per million (ppm) (*2*, *3*), the highest of the past 420 million years (Ma) (*4*). Despite modeling results indicating freezing winter temperatures at high latitudes (*5*, *6*), empirical evidence for freezing has been lacking. Here, we provide empirical evidence showing that, despite extraordinary high P_{CO_2}, freezing winter temperatures did characterize high Pangean latitudes based on stratigraphically widespread lake ice-rafted debris (L-IRD) in early Mesozoic strata of the Junggar Basin, northwest China (Figs. 1 and 2 and fig. S1). Traditionally, dinosaurs have been viewed as thriving in the warm and equable early Mesozoic climates, but our results indicate that they also endured freezing winters. We argue that the rich plant resources of the high latitudes were key for the survival of early herbivorous dinosaurs and that insulated dinosaurs were well adapted to these cold conditions. Adaptation to cold accounts for their success at the expense of large noninsulated reptiles during the volcanic winters of the Central Atlantic Magmatic Province (CAMP) that marked the end-Triassic extinction (ETE), one of largest mass extinctions of all time (*7*).

RESULTS

Late Triassic–Early Jurassic high-latitude L-IRD

Late Triassic and Early Jurassic strata of the Junggar Basin were deposited north of the Arctic Circle at about 71°N paleolatitude (Fig. 1; see the "Methods" section in Materials and Methods and fig. S1) and consist of cyclical, coal-bearing, fluvial, and lacustrine rocks of the Huangshanjie, Haojiagou, Badaowan, and Sangonghe formations (fig. S3). Within these strata, the ETE and Triassic-Jurassic boundary are in the basal Badaowan Formation. Multiple, lacustrine dark gray and black fine-grained (~0.1 to 63 μm) thin-bedded laterally continuous lacustrine mudstone beds at multiple localities in the Huangshanjie, Haojiagou, and Badaowan formations contain dispersed 0.1- to 15-mm lithic grains (see the Supplementary Materials). Some of these beds also contain bivalve mollusks, clam shrimp, isolated to partially disarticulated fish remains, and tetrapod fragments. Quantitative granulometry of these layers with outsized clasts shows a characteristic bimodal grain size distribution (Fig. 2) that, in pelagic marine strata, is attributed to IRD (see the Supplementary Materials) (*8*), a property also visible in hand samples (fig. S1 and table S1). In lakes, as in marine environments not dominated by glacial input, such as the Sea of Okhotsk (Fig. 2 and fig. S2), the origin of this IRD is seasonal ice that freezes along the shoreline, seizes grains in contact with the bottom, and then drifts out into open water when it breaks up and melts. Grains that may have saltated or were strewn across the frozen surface as well as eolian dust can also contribute (*9*). L-IRD have been used as surface ice proxy in Quaternary

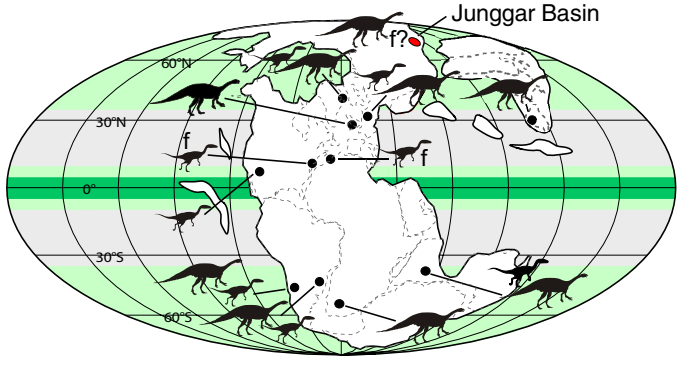

Fig. 1. Pangaea at 202 Ma (Mollweide projection) showing location of Junggar Basin (fig. S1) and Triassic dinosaurs. Data for dinosaurs are from (*18*, *64*, *77*, *78*) and herein for Junggar. f denotes occurrences based on footprints data alone (*64*), large silhouettes are herbivores, and smaller ones are small- to medium-sized carnivorous theropods. Modified from (*18*).

[1]Lamont-Doherty Earth Observatory, Columbia University, Palisades, NY 10968, USA. [2]State Key Laboratory of Palaeobiology and Stratigraphy, Nanjing Institute of Geology and Palaeontology, Chinese Academy of Sciences, Nanjing 210008, China. [3]School of Ocean and Earth Sciences, National Oceanography Centre, University of Southampton, Southampton SO14 3ZH, UK. [4]Department of Paleobiology, National Museum of Natural History, Smithsonian Institution, Washington, DC 20013-7012, USA. [5]Earth and Planetary Sciences, Rutgers University, Piscataway, NJ 08854, USA. [6]Earth and Environmental Sciences, Rensselaer Polytechnic Institute, Troy, NY 12180, USA. [7]Department of Palaeobiology, Swedish Museum of Natural History, Stockholm, Sweden. *Corresponding author. Email: jgsha@nigpas.ac.cn (J.S.); polsen@ldeo.columbia.edu (P.O.)

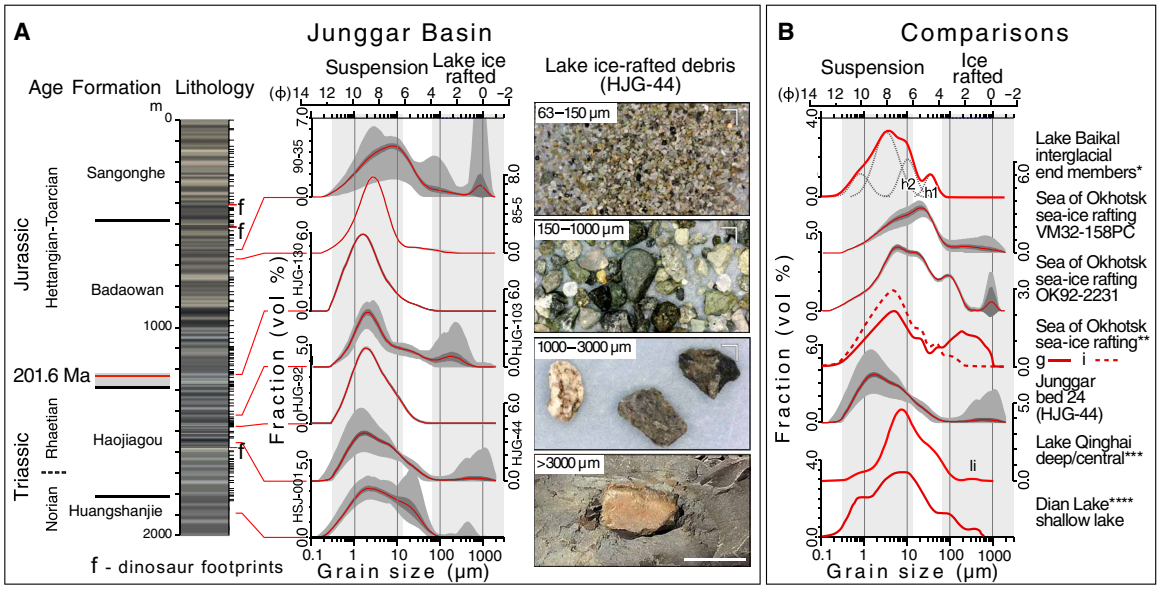

Fig. 2. Comparison of granulometry results from the Junggar Basin lacustrine intervals with L-IRD and some without compared to results from select modern bodies of water with and without seasonal IRD (sources of data from non-Junggar Lake in the Supplementary Materials). (**A**) Granulometry and examples of L-IRD from the Junggar Basin. Left: Section is based from (*16*) and a modified Google Earth image of the Haojiagou section (fig. S1). Middle: Quantitative lasersizer granulometry results of Junggar mudstone samples, with the mean (red line), the 95% confidence limits (dark gray envelope), and the range (light gray envelope) of repeated aliquots shown (details in the Supplementary Materials). Right: 63- to 3000-μm–sieved L-IRD from sample HGJ-44 of bed 24, >3000-μm example, is a field photograph; scale is 1 cm (details in the Supplementary Materials, fig. S5, movie S1, and tables S1 and S2). (**B**) Quantitative lasersizer granulometry comparisons between known IRD and material from the Junggar Basin (locations for Sea of Okhotsk in fig. S2 and table S1): *Four–end-member model for the grain size distribution data, Lake Baikal; h1 and h2, hemipelagic sediment-modified low-energy bottom currents (other Baikal cores have L-IRD of possible mountain glacier origin; see the Supplementary Materials); **typical examples of glacial (g) and interglacial (i) sediment from the Sea of Okhotsk (*8*); ***Lake Qinghai sediments from the deep/central basin with L-IRD (li); ****Dian Lake shallow/transitional lake zone with wave reworking of sediment and therefore has a much more continuous distribution of grain sizes. Photo credit: Clara Chang, Sean Kinney, and Paul Olsen, LDEO, Columbia University.

lake deposits (*9*–*11*) and are distinct from other potential sources of rafted grains (see the Supplementary Materials). However, not all sediments from lakes with seasonal ice exhibit L-IRD (Fig. 2), for reasons that are as yet unclear. We therefore illustrate examples of sediment cores from water bodies with and without L-IRD that exhibit seasonal freezing in Fig. 2 to compare with the Junggar lacustrine strata showing similar variations in L-IRD. Shallow water, siltstones, and sandstone beds interbedded with rooted intervals in all three Triassic-Jurassic formations studied here produce dinosaur footprints (see the Supplementary Materials and fig. S4) (*12*), demonstrating that dinosaurs were present at these arctic latitudes associated with freezing winter temperatures as background climatic conditions. This is consistent with available climate models that consistently show freezing wintertime temperatures in high-latitude Asia for the Late Triassic and Jurassic (*5*, *6*, *13*, *14*) and congruous with models for Mesozoic climate until extremely high P_{CO_2} levels (e.g., 4480 ppm) are reached (*15*). However, despite these models, warm arctic conditions have been asserted by some on the basis of equivocal proxy data, e.g., an assessment possible in the absence of empirical evidence of arctic freezing, such as these L-IRD. Although seasonal freezing is indicated by our results, none of our data require the presence of perennial ice, ice sheets, or glaciers, although they are not ruled out.

Early Mesozoic strata of the Junggar Basin are cyclical and paced largely by strong obliquity as well as precessional insolation (Milankovitch) cycles (*16*). These L-IRD provide a potential proxy for such cyclicity because the presence of at least some lacustrine strata without L-IRD (Fig. 2) suggests warmer interludes without wintertime freezing.

Triassic dinosaurian latitudinal zonation

Freezing temperatures in the forested high latitudes of the Triassic-Jurassic have implications for the distribution of contemporaneous tetrapods. While an ambitious cursorial tetrapod could conceivably have walked from nearly pole to pole, the composition of tetrapod communities was markedly latitudinally zonal (*14*, *17*, *18*), especially so for herbivorous dinosaurs (Fig. 1). Unlike the modern world, the highest-diversity continental assemblages were in the midlatitudes (*14*). The oldest definitive evidence for dinosaurs (both carnivores and herbivores) (*19*) is from the Carnian age (~231 Ma) Ischigualasto Formation at 48°S paleolatitude (*20*). By the middle to late Norian (~215 Ma), large (5 to 10 m) herbivorous basal sauropodomorph dinosaurs ("prosauropods") were common at midlatitudes (~24° to 60°) in both hemispheres, but continental tetrapod assemblages from the coal-bearing high latitudes have been virtually unknown (*18*, *21*).

In contrast, Norian assemblages from low paleolatitudes lack herbivorous dinosaurs, while nondinosaurian and non-archosaurian archosauromorphs, especially the semiaquatic phytosaurs and diverse pseudosuchians, including herbivorous forms, are dominant (*14*). While generally small carnivorous dinosaurs were present, they comprised a relatively minor part of low-latitude communities (*18*).

Most of the temnospondyl amphibians of the midlatitudes also differ from those of low latitudes (*22*). In summary, large dinosaurian herbivores were restricted to higher latitudes (Fig. 1).

Plants also show a very strong latitudinal zonation (*23*). The equatorial tropics had floral assemblages dominated by conifers, seed ferns, and ferns, at least during wet periods of climate cycles, and many groups have extant representatives that are intolerant to freezing. The semiarid tropics and subtropics had lower-diversity assemblages dominated by conifers, while midlatitude assemblages have much higher-diversity floras. The forests of the high northern latitudes (>60°) as in northwestern China had abundant deciduous, relatively large-leafed conifers, *Podozamites* (*24*), gingkoes, and other deciduous plants (*25*), and trees with wood with well-developed growth rings (*26*), consistent with a cool to cold winter climate, perhaps with some warmer interludes (see the Supplementary Materials). This zonation is strongly reflected in the pollen and spore assemblages. Despite an apparent lack of geographic barriers, many taxa are restricted to particular latitudinal belts, where some dominant forms in the tropics and subtropics, such as *Patinasporites*, are absent from high latitudes (*27*, *28*), while some key taxa of the midlatitudes, such as *Rhaetipollis*, are absent from the tropics (*28*).

Physiologically relevant characters map to geographic distributions

We use a generalized phylogenetic bracket approach (*29*) based on preserved soft tissue features of extinct tetrapods as well as soft tissue and physiological traits from extant taxa to infer traits in specific extinct groups in which soft tissue features and physiological traits are not preserved (Fig. 3 and the Supplementary Materials). The most important of these are as follows: (i) Nearly all present-day reptiles are uricotelic (*30*) (synthesizing and excreting uric acid) and thus conserve water. This was the case for basal dinosaurs as well as terrestrial nondinosaurian Archosauriformes and is a highly advantageous trait in hot and water-stressed environments. (ii) Given that filamentous integumentary coverings ("protofeathers") were widespread in several clades of non-avian theropod dinosaurs (*31*), including large-bodied ones (*32*), and in at least two clades of basal, small-bodied plant-eating ornithischian dinosaurs (*33*), it is reasonable to hypothesize that integumentary covers were primitive for dinosaurs. Furthermore, these fossils also show that these protofeathers evolved in animals that were never capable of flight. The filamentous integumentary structures of pterosaurs (*34*) are most parsimoniously interpreted as homologous to those in dinosaurs, and if that is the case, such structures were primitive for Avemetatarsalia in general as was small body size (*34*–*36*). We argue that the simplest functional hypothesis for these integumentary structures is that they served for thermal insulation. The apparent lack of protofeathers or feathers in known large sauropodomorphs in which integument is at least partially preserved and some large-bodied theropods may be related to their body size in warm climates (*32*, *37*) and their need to dissipate rather than retain heat, just as adult African elephants lack fur. The minimal interpretation of the distribution of integumentary filaments is that they served for insulation and were a primitive character at the level of pterosaurs plus dinosaurs and plausibly the entire Avemetatarsalia (*34*, *38*). This is the most parsimonious deduction that can be made, even if the resurrected Ornithoscelida (*39*) hypothesis (with ornithischians as the sister group of theropods, excluding sauropodomorphs) proves most parsimonious for dinosaur phylogeny (see the Supplementary Materials). In addition, non-avian dinosaurs, while showing a variety of growth strategies, tended to exhibit high growth rates and features indicative of high, if variable, metabolic levels (*40*) compared to most, if not all (*41*),

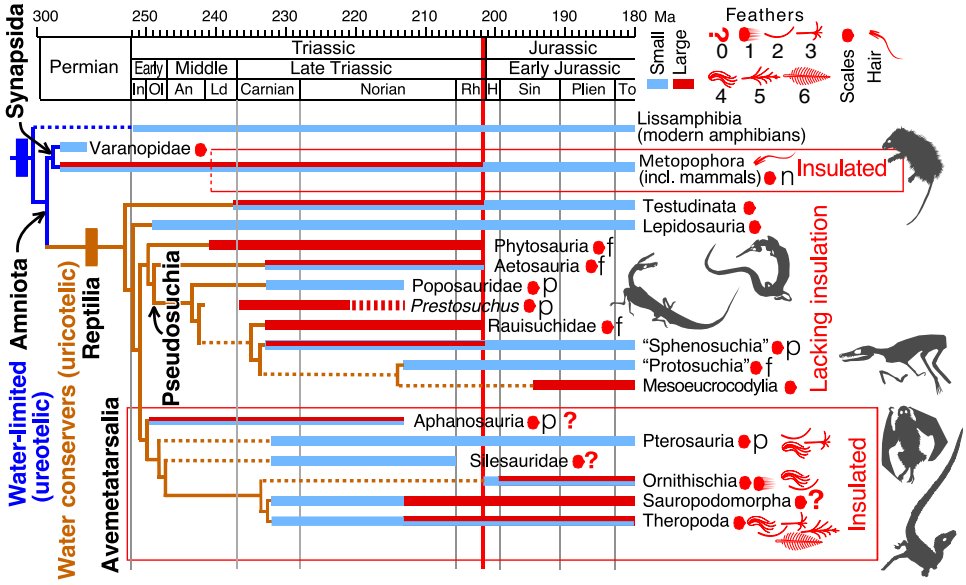

Fig. 3. Cladogram of physiologically important characters on phylogenetic framework. Feather type 1 is a bristle scale; feather types 2 to 6 include protofeathers based on extant groups (birds) and fossil occurrences in which integumentary strictures are preserved; feather type 0, represented by a question mark, is a prediction that protofeathers for insulation should be primitively present but what form they should take is unknown. For scales, abbreviations are as follows: f, scales are present on the feet based on footprints assigned to that taxon; p, scales are predicted by the phylogenetic bracket approach; n, scale-like structures in some mammaliaformes of uncertain homology. The clade Metopophora consists of all those synapsids more closely related to *Homo* than the Varanopidae. Details of sources are in the Supplementary Materials.

non-avemetatarsalian reptiles. This hypothesis depends only on the homology of the filamentous integument of pterosaurs [pycnofibers (*42*)] to protofeathers (*43*) and in having the Pterosauria as a basal sister group to the Dinosauria, which is currently the most parsimonious hypothesis.

These physiological and morphological attributes correlate to geographical regions during the Triassic via the following scenario: The absence of large herbivorous dinosaurs and the dominance of pseudosuchians, both carnivores and herbivores, in the Late Triassic tropics (*18*) suggest that herbivorous dinosaurs could not compete with herbivorous pseudosuchians. Although both groups were uricotelic water conservers based on ancestral state reconstruction (Fig. 3), the absence of herbivorous dinosaurs may be related to the apparent highly variable and unpredictable floral resources in at least most of the tropics, which made the herbivorous dinosaurs with their high metabolic rates incapable of establishing viable populations, while the lower metabolic requirement pseudosuchian herbivores could thrive (*18*), albeit at a smaller maximum body size.

In contrast, at mid- and higher latitudes, herbivorous pseudosuchians were less common than herbivorous basal sauropodomorphs (*14*, *18*). While preserved integument has yet to be found in these dinosaurs, which were much smaller than the giant sauropods known to be largely scaly, they are predicted to be insulated by our phylogenetic bracket approach. Such insulation would have allowed them to take advantage of the abundant and more stable floral resources at high paleolatitudes. We predict that large pseudosuchians, for which there is no evidence of such insulation, will prove to be absent in colder high latitudes, especially with freezing winter temperatures. This is despite the possibility that basal crocodylomorphs or other pseudosuchians may have been endothermic with high growth rates [e.g., (*41*)]. We hypothesize that insulation and endothermy were key advantages for Triassic herbivores, just as they permit modern temperate, boreal herbivores to take advantage of the deciduous vegetation in the summer and evergreen vegetation in the winter. However, endothermy without insulation, as might have been the case for at least some large pseudosuchians, would be a liability, not an advantage, in the cold.

Volcanic winters caused the terrestrial ETE

Atmospheric P_{CO_2} was extremely high during most of the early Mesozoic (>2000 ppm), particularly during the Late Triassic and earliest Jurassic (~232 to 199 Ma) (Fig. 4) (*2*, *3*, *44*, *45*). However, there was a substantial decline (<2000) during the early and middle Rhaetian (205.7 to 201.6 Ma) associated with a decrease in ocean temperatures (*2*, *46*). During this time, dinosaurian abundance and size increased in the tropics, although apparently only theropods were present (*18*).

The pulsed eruptions of the CAMP were associated with abrupt doubling to tripling of P_{CO_2} before which P_{CO_2} had dropped from its earlier zenith (*44*, *45*). On the basis of modeling for anthropogenic P_{CO_2} climate sensitivity, the CAMP-related increases would be expected to produce ~3° to 5°C (or higher) increases in average global temperatures (*4*, *47*) from the Rhaetian background. While abrupt P_{CO_2} increases are clearly implicated in the marine invertebrate extinctions due to ocean acidification and anoxia (*48*, *49*), the predicted effects on land would seem to be at odds with the climatic consequences of very high volcanic CO_2. An increase in temperatures on land should be expected to drive mid- to high-latitude tetrapods poleward as seems to be the case with some plants (*50*). In contrast,

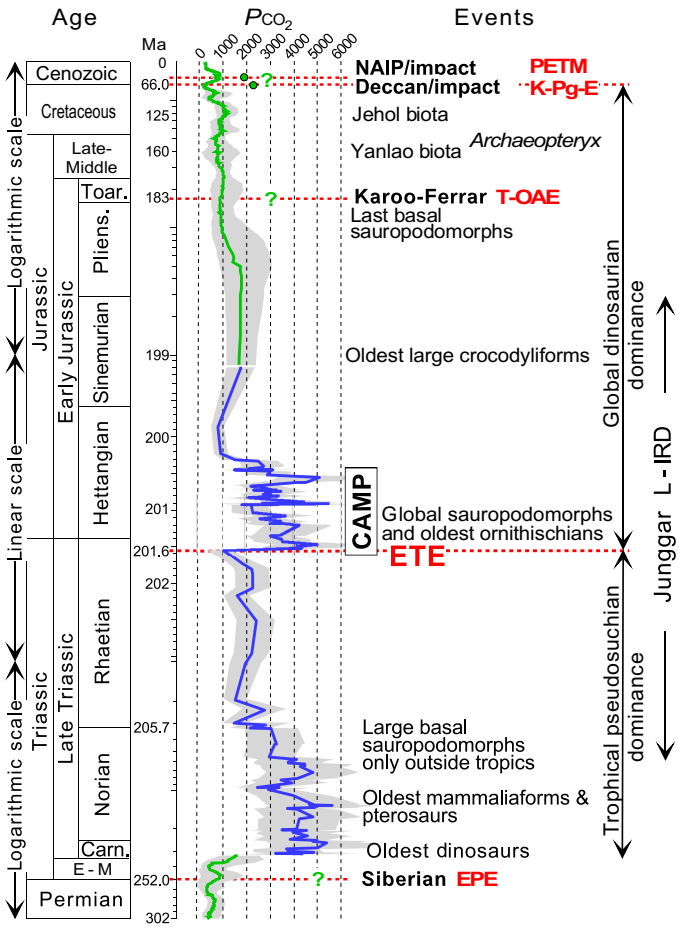

Fig. 4. Timeline for the dinosaurian ecological takeover showing relationship among CAMP, P_{CO_2}, L-IRD, extinction of large tropical pseudosuchians (including their large uninsulated relatives), and the rise of global dinosaurian ecological dominance. Note that the time scale is logarithmic for times younger than 199 Ma and older than 201.4 Ma. For P_{CO_2}, blue is based on soil carbonate proxy (*2*, *45*) and green is based on a compilation of multiple proxies (*4*). PETM, Paleocene-Eocene thermal maximum; K-Pg, Cretaceous-Paleogene boundary; T-OAE, Toarcian anoxic event; ETE, end-Triassic extinction; EPE, end-Permian extinction.

members of higher-latitude tetrapod assemblages disproportionately survived and migrated into the tropics, most notably basal sauropodomorph dinosaurs that only then appear in North America (*51*), and thus, on land, extinction selectivity is more consistent with cold, specifically CAMP-induced volcanic winters.

Volcanic winters (*52*), the term for the devastating cooling caused by volcanic sulfur aerosols, are well documented for historical and older eruptions (*53*, *54*). Cooling from sulfur aerosols has been proposed as a contributor to the ETE [e.g., (*55*)]; there is plant physiognomic and cuticular evidence for damaging increased sulfur aerosols during that event (*56*, *57*) and an increase in plants adapted to low light levels such as ferns (both spores and macrofossils) (*58*). Volcanic winters through the ~1 Ma bracketing the Triassic-Jurassic transition were plausibly extreme and long in duration (>10 years). Individual flows were thousands of cubic kilometers in volume, perhaps the products of prolonged, even decade-long eruptions that were two orders of magnitude larger than any historical eruptions (*59*). Thus, even if the atmosphere saturated with respect to aerosols,

the sustained eruptions with related pulses of sulfur would have caused decade-long volcanic winters. CAMP emplacement was pulsed at the hundred-thousand-year scale (*44*, *45*, *60*), with each pulse consisting of several individual gigantic eruptions, with the consequences enhanced because the CAMP emplacement straddled the equator. Climate modeling specifically for the CAMP and ETE suggests that the drops in temperature from volcanic sulfur aerosols were much larger than the increases due to CO_2 warming, although much shorter in duration (*61*). Sustained temperature drops in excess of 10°C (*61*) were possible, perhaps resulting in multiple events of tropical freezing similar, although not as large in magnitude as modeled for the aerosols of the K-Pg impact (Fig. 4) (*62*).

DISCUSSION

From their discovery, dinosaurs have been conceptually associated with tropical or at least warm climates (*63*). This idea is antithetical to them inhabiting the high latitudes with freezing winters or their survival through episodes of volcanically induced winters. Empirical evidence of L-IRD in strata associated with dinosaur footprints shows that these insulated archosaurs lived in areas and in times with freezing conditions since their inception in the Late Triassic. In contrast, the tropical large terrestrial archosauromorphs of the Triassic, including phytosaurs and pseudosuchians, lacked insulation and presumably could not tolerate prolonged cold, let alone persistent freezing. Thus, large-bodied (>1 m) terrestrial archosauromorphs went extinct during the initial CAMP eruptions at the ETE. This is markedly shown by both skeletal and footprint data from the paleotropics (*64*). Of pseudosuchians, only small-bodied basal crocodylomorphs survived the ETE and only the small (2 to 3 cm) pseudosuchian track taxon *Batrachopus* has been found in post-ETE Rhaetian and Hettangian strata. These small-bodied forms also lacked insulation but could have survived in burrows during volcanic winters, as uninsulated forms (e.g., turtles) do now where there are freezing winters, and as has been proposed for survival through the K-Pg event (*65*). Overall, archosauromorphs show no size selectivity through the extinction (*66*), although they do when parsed into insulated versus noninsulated clades (Fig. 3). Crocodylomorphs did not reoccupy the continental semiaquatic phytosaurian niche until millions of years later (*67*).

There is, however, little or no evidence of extinction among dinosaurian clades during the ETE; they underwent an expansion in maximum size and geographic range (Fig. 4). Basal sauropodomorphs, abundant at mid- and higher latitudes during the Late Triassic, spread into the tropics (*28*), definitive ornithischians appear for the first time (*28*, *68*), and the maximum size of theropods (at least in the tropics) increased by 20% (*64*), equating to nearly a doubling of mass. The climatic consequences of the doublings to triplings of CAMP input of CO_2 that took tens to hundreds of thousands of years to dissipate (*2*, *44*, *45*) seem an inadequate explanation for the selectivity of the extinctions on land. This is especially true in light of the fact that both dinosaurs and the victims of the CAMP were similarly uricotelic and adapted to water stress. The terminal Triassic, abrupt CAMP-related increase in P_{CO_2} stands out as unusual largely because it was preceded by a drop in P_{CO_2} in the earlier Rhaetian (*2*), yet large-sized pseudosuchians and non-archosaurian archosauromorphs that were dominant in the tropics during the preceding 30 Ma nearly vanished during the end-Triassic. The darkness and cold of volcanic winters seems a far more parsimonious explanation of the selectivity of the extinction as opposed to a comparatively small increase in average temperatures that could have been mitigated by poleward or altitudinal migration.

Even as it has become clear that many dinosaurs were insulated with protofeathers, the idea that non-avian dinosaurs were predominately denizens of warm climates in an ice-free high P_{CO_2} hothouse Mesozoic world has persisted. It is now apparent here based on empirical evidence (rather than just models) that freezing temperatures occurred seasonally at high latitudes during the Late Triassic and Early Jurassic despite exceptionally high P_{CO_2}. Being primitively insulated, dinosaurs were able to take advantage of the rich plant resources in the high latitudes. Through their adaptation to cold temperatures, dinosaurs were able to survive the CAMP volcanic winters and thereby expand to dominate terrestrial communities for the next 135 Ma, and, as birds, remain two to three times more speciose than mammals to this day (*69*, *70*).

MATERIALS AND METHODS

Junggar Basin materials

Outcrop samples from Haojiagou were collected by conventional means (i.e., with pick and rock hammer), generally in a shallow trench to a depth of 10 to 30 cm to below the visually weathered zone. Locations of the sedimentary successions and sampling sites are shown in fig. S1 and table S1. Core samples were recovered from piston core VM32-158PC archived at the Lamont-Doherty Earth Observatory (LDEO) and gravity core OK92-2231 (fig. S2) archived at the Oklahoma State University (table S1). Approximately 5 cm^3 of sediment from each of the cores was subsampled for grain size analysis. IGSN (International Generic Sample Number) identifiers for these samples are provided in table S1.

Dinosaur footprints have been found in the Sangonghe, Haojiagou, and Badaowan formations. In the Sangonghe Formation, footprints were found in the Haojiagou area outcrops, bed 110, NIGPAS (Nanjing Institute of Geology and Paleontology Academy of Science) PB172137 (latitude: 43.67486°, longitude: 87.20023°) (fig. S4A), with the figured specimen consisting of a natural cast (convex hyporelief) of a tridactyl footprint in tan (as weathered) fine sandstone. Its relatively high angulation and relatively short digit III, given its small size, suggests an ornithischian track, although this is not conclusive. Underlying strata show typical "dinoturbation" (fig. S4B), which was the clue that resulted in the recovery of PB172137. No additional footprints were excavated or collected at this site because of logistical issues related to their fragility and preservation. Badaowan Formation footprints were found by our team at the Haojiagou outcrops, bed 98, but not collected because of size (latitude: 43.67141°, longitude: 87.20398°). This track consists of a partial tridactyl natural cast (convex hyporelief) (fig. S4D) found as float on a small promontory capped by appropriate lithology, making its provenance certain. Although it has a high angulation, its larger size and penetrative mode of formation make assignment to a specific dinosaur group speculative. In addition, a previously collected specimen from the Badaowan Formation was collected at the Wanminggou tracksite (latitude: 44.13889°, longitude: 84.28028°, about 233 km west-northwest of the Haojiagou outcrops, NIGPAS MV11) (*12*). It is a natural cast (convex hyporelief) of a nearly complete right pes impression with another track anterior to it that is a possible manus. Originally reported as cf. *Changpeipus* sp. by Xing *et al.* (*12*), based on its small size of 10.7 cm, short digit III, wide digital divarication, and metatarsal-phalangeal pad of digit IV

in line with the axis of digit III, this track seems a better fit to *Anomoepus* [criteria from (*71*)], the track of an herbivorous ornithischian dinosaur. The Haojiagou Formation at the Haojiagou outcrops, bed 24 (not collected) (latitude: 43.64571°, longitude: 87.20510°), shows another example of dinoturbation (fig. S2D). These footprints were not excavated or collected at this site because of logistical issues related to their fragility and preservation, and therefore, assignment to a specific dinosaur group is speculative.

Methods

Paleolatitude determination

Paleoclimatically useful continental reconstructions for the Mesozoic and Cenozoic are based on plate kinematics from the sea-floor record extrapolated back to closure and within a paleolatitudinal framework that is based on the assumption that the time-averaged geomagnetic field closely approximates that of a geocentric axial dipole (GAD) such that those paleomagnetic poles that faithfully record the GAD are good approximations of Earth's rotation axis [e.g., (*72*)]. Here, we use a 200-Ma mean pole using data from North America, Eurasia, South America, and Africa to position the major continental assembly of Pangaea at around the time of the ETE and Triassic-Jurassic boundary at ~200 Ma (*73*). Our working hypothesis is that the Junggar and Tarim basins were already effectively docked with respect to Siberia (*74*), and Siberia was part of Eurasia by the end of the Permian. That being the case, we can rotate reported 200-Ma mean poles to Siberian coordinates using standard reconstruction parameters for the Atlantic-bordering continents and use that 200-Ma pole to estimate the paleolatitude of the Triassic-Jurassic southern Junggar Basin sampling site located today at 43.7°N, 87.2°E. As detailed in the Supplementary Materials and supported by other syntheses, this 200-Ma pole gives a paleolatitude of 71.1° ± 3.8°N for the sampling site in the Junggar Basin.

Quantitative granulometry (grain size analysis) sample preparation

Junggar sample preparation consisted of three steps. (i) Disaggregation and removal of organic material, pyrite, and carbonate cement: We weighed out 10 to 20 g of rock, covered them with 30% H_2O_2, and warmed them on a 50°C hot plate for >3 weeks. Additional 30% H_2O_2 was added as needed. In this process, peroxide also oxidized the organic material. Oxidation of pyrite forms H_2SO_4 that also dissolved the carbonate cement. Initial tests using sonication to break up the sample indicated that the carbonate was restricted to matrix cement, and no carbonate clasts were present that would be dissolved. The coarse fraction was inspected using light microscopy to verify total disaggregation. In cases where samples were not disaggregated within 3 weeks, additional 20% HCl was added, reacted overnight, centrifuged, and rinsed. Then, 30% H_2O_2 was added to remove the newly liberated organics. Samples were rinsed and centrifuged three times with deionized (DI) water. (ii) Charcoal removal: Saturated zinc chloride solution was added to each sample and centrifuged to float out charcoal and other recalcitrant organics, which were pipetted off. This process was repeated until there was no visible charcoal left in the sample. Samples were rinsed and centrifuged three times with DI water. (iii) Sieving: Subsamples of disaggregated HJG-44, HJG-103, and HJG-130 were sieved at 63 to 150, 150 to 250, 250 to 500, 500 to 1000, and >1000 μm (table S2), with results expressed as weight percent relative to the whole rock.

Sea of Okhotsk sample preparation consisted of removal of organic material, carbonate microfossils, and biogenic silica. Samples were heated, sonicated, and reacted overnight, first with 5% H_2O_2 to remove organics, then 10% HCl to remove carbonate, and finally 2 M $NaCO_3$ to remove biogenic silica, as described in (*8*, *75*). Samples were centrifuged and rinsed three times with DI water.

Laser diffraction granulometry

Quantitative granulometry (grain size analysis) was conducted using laser diffraction with Malvern Mastersizer 2000 and 3000. We used a standard reference material and subsampled the sample to exhaustion as detailed in the Supplementary Materials. (i) Samples were sieved at 2 mm to remove the largest grains that would damage the lasersizer. The Malvern software uses Mie theory to convert light energy scatter to grain size and reports grain size distributions as volume percentages. The fine fraction data are demonstrably precise and accurate and show extremely high reproducibility. The coarse fraction is more variable, reflecting the small numbers of larger particles in different pipetted aliquots of the same sample, which was compensated by sampling to exhaustion. Visual inspection of the rock samples, thin section, and a computed tomography (CT) scan (movie S1) as well as sieving (Fig. 2 and table S2) confirm that the quantitative results reflect a real coarse fraction component in these samples. The mean and 95% confidence limits were calculated, and these, along with the range of the data, are shown in Fig. 2.

CT scan

Samples were scanned at Yale University on a Nikon XT H 225 ST by B.-A. Bhuller. The resolution was 0.023883 mm. Image stacks were produced with VGSTUDIO, and the three-dimensional projection was generated with ImageJ.

Thin section

A thin section (fig. S4 and table S1) was prepared from the same piece of mudstone of HJG-44 as used for the CT scan (movie S1 and table S1) by Wagner Petrographic (UT, USA) and is a standard thin section of 26 mm × 44 mm with a thickness of 30 μm. A clear epoxy mount was used, and the sample was double-polished. Photographs were taken with a Keyence digital microscope with transmitted light.

Phylogenetics

We used generalized phylogenetic bracket analysis (*29*) to infer traits in clades for which there is no physical evidence (see the Supplementary Materials for details). We mapped preserved soft tissue features of extinct tetrapods as well as soft tissue and physiological traits from extant taxa onto an existing cladogram, allowing the inference of traits in specific extinct groups in which soft tissue features and physiological traits are not preserved. The phylogenetic results of Nesbitt (*76*) were used as the base tree on which the known integumentary and physiological traits were plotted (Fig. 3). Details are in the Supplementary Materials.

SUPPLEMENTARY MATERIALS

Supplementary material for this article is available at https://science.org/doi/10.1126/sciadv.abo6342

REFERENCES AND NOTES

1. L. A. Frakes, J. E. Francis, J. I. Syktus, *Climate Modes of the Phanerozoic: The History of the Earth's Climate Over the Past 600 Million Years* (Cambridge Univ. Press, 1992), p. 274.
2. M. F. Schaller, J. D. Wright, D. V. Kent, A 30 Myr record of Late Triassic atmospheric pCO_2 variation reflects a fundamental control of the carbon cycle by changes in continental weathering. *Geol. Soc. Am. Bull.* **127**, 661–671 (2015).
3. J. C. McElwain, D. J. Beerling, F. I. Woodward, Fossil plants and global warming at the Triassic-Jurassic boundary. *Science* **285**, 1386–1390 (1999).
4. G. L. Foster, D. L. Royer, D. J. Lunt, Future climate forcing potentially without precedent in the last 420 million years. *Nat. Commun.* **8**, (2017).
5. B. W. Sellwood, P. J. Valdes, Jurassic climates. *Proc. Geol. Assoc.* **119**, 5–17 (2008).

6. J. Landwehrs, G. Feulner, S. Petri, B. Sames, M. Wagreich, Investigating Mesozoic climate trends and sensitivities with a large ensemble of climate model simulations. *Paleoceanogr. Paleoclimatol.* **36**, e2020PA004134 (2021).
7. M. J. Benton, Diversification and extinction in the history of life. *Science* **268**, 52–58 (1995).
8. T. Sakamoto, M. Ikehara, K. Aoki, K. Iijima, N. Kimura, T. Nakatsuka, M. Wakatsuchi, Ice-rafted debris (IRD)-based sea-ice expansion events during the past 100 kyrs in the Okhotsk Sea. *Deep Sea Res. Part II Top. Stud. Oceanogr.* **52**, 2275–2301 (2005).
9. G. Fedorov, A. A. Andreev, E. Raschke, V. Wennrich, G. Schwamborn, O. Y. Glushkova, O. Juschus, A. Zander, M. Melles, Middle to Late Pleistocene lake-level fluctuations of Lake El'gygytgyn, far-east Russian Arctic. *Boreas* **48**, 516–533 (2019).
10. S. R. Zimmerman, C. Pearl, S. R. Hemming, K. Tamulonis, N. G. Hemming, S. Y. Searle, Freshwater control of ice-rafted debris in the last glacial period at Mono Lake, California, USA. *Quatern. Res.* **76**, 264–271 (2011).
11. C. A. Jessen, M. Rundgren, S. Björck, C. S. Andresen, D. J. Conley, Variability and seasonality of North Atlantic climate during the early Holocene: Evidence from Faroe Island lake sediments. *Holocene* **18**, 851–860 (2008).
12. L.-D. Xing, M. G. Lockley, W. Qi-Fei, L. Zhong-Dong, H. Klein, W. Scott Persons IV, Y. Yong, M. Matsukawa, Earliest records of dinosaur footprints in Xinjiang, China. *Vertebrata PalAsiatica* **52**, 340–348 (2014).
13. B. W. Sellwood, P. J. Valdes, Mesozoic climates: General circulation models and the rock record. *Sediment. Geol.* **190**, 269–287 (2006).
14. E. M. Dunne, A. Farnsworth, S. E. Greene, D. J. Lunt, R. J. Butler, Climatic drivers of latitudinal variation in Late Triassic tetrapod diversity. *Palaeontology* **64**, 101–117 (2021).
15. W. W. Hay, R. M. DeConto, P. de Boer, S. Flögel, Y. Song, A. Stepashko, Possible solutions to several enigmas of Cretaceous climate. *Int. J. Earth Sci.* **108**, 587–620 (2019).
16. J. Sha, P. E. Olsen, Y. Pan, D. Xu, Y. Wang, X. Zhang, X. Yao, V. Vajda, Triassic-Jurassic climate in continental high-latitude Asia was dominated by obliquity-paced variations (Junggar Basin, Ürümqi, China). *Proc. Natl. Acad. Sci. U.S.A.* **112**, 3624–3629 (2015).
17. J. H. Whiteside, D. S. Grogan, P. E. Olsen, D. V. Kent, Climatically driven biogeographic provinces of Late Triassic tropical Pangea. *Proc. Natl. Acad. Sci. U.S.A.* **108**, 8972–8977 (2011).
18. J. H. Whiteside, S. Lindström, R. B. Irmis, I. J. Glasspool, M. F. Schaller, M. Dunlavey, S. J. Nesbitt, N. D. Smith, A. H. Turner, Extreme ecosystem instability suppressed tropical dinosaur dominance for 30 million years. *Proc. Natl. Acad. Sci. U.S.A.* **112**, 7909–7913 (2015).
19. S. L. Brusatte, M. J. Benton, M. Ruta, G. T. Lloyd, Superiority, competition, and opportunism in the evolutionary radiation of dinosaurs. *Science* **321**, 1485–1488 (2008).
20. D. V. Kent, L. B. Clemmensen, Northward dispersal of dinosaurs from Gondwana to Greenland at the mid-Norian (215–212 Ma, Late Triassic) dip in atmospheric pCO_2. *Proc. Natl. Acad. Sci. U.S.A.* **118**, e2020778118 (2021).
21. H.-D. Sues, *Arctosaurus osborni*, a Late Triassic archosauromorph reptile from the Canadian Arctic Archipelago. *Can. J. Earth Sci.* **54**, 129–133 (2017).
22. N. H. Shubin, H. D. Sues, Biogeography of early Mesozoic continental tetrapods: Patterns and implications. *Paleobiology* **17**, 214–230 (1991).
23. E. Kustatscher, S. R. Ash, E. Karasev, C. Pott, V. Vajda, J. Yu, S. M. Loughlin, in *The Late Triassic World: Earth in a Time of Transition*, L. H. Tanner, Ed. (Springer, 2018), chap. 13, pp. 545–622.
24. M. Pole, Y. Wang, E. V. Bugdaeva, C. Dong, N. Tian, L. Li, N. Zhou, The rise and demise of *Podozamites* in east Asia—An extinct conifer life style. *Palaeogeogr. Palaeoclimatol. Palaeoecol.* **464**, 97–109 (2016).
25. G. Sun, Y. Miao, V. Mosbrugger, A. R. Ashraf, The Upper Triassic to Middle Jurassic strata and floras of the Junggar Basin, Xinjiang, Northwest China. *Paleobiodivers. Paleoenviron.* **90**, 203–214 (2010).
26. M. Wan, W. Zhou, P. Tang, L. Liu, J. Wang, *Xenoxylon junggarensis* sp. nov., a new gymnospermous fossil wood from the Norian (Triassic) Huangshanjie Formation in northwestern China, and its palaeoclimatic implications. *Palaeogeogr. Palaeoclimatol. Palaeoecol.* **441**, 679–687 (2016).
27. P. A. Hochuli, J. O. Vigran, Climate variations in the Boreal Triassic—Inferred from palynological records from the Barents Sea. *Palaeogeogr. Palaeoclimatol. Palaeoecol.* **290**, 20–42 (2010).
28. P. E. Olsen, D. V. Kent, J. H. Whiteside, Implications of the Newark Supergroup-based astrochronology and geomagnetic polarity time scale (Newark-APTS) for the tempo and mode of the early diversification of the Dinosauria. *Earth Environ. Sci. Trans. R. Soc. Edinb.* **101**, 201–229 (2010).
29. L. M. Witmer, in *Functional Morphology in Vertebrate Paleontology,* J. J. Thomason, Ed. (Cambridge Univ. Press, 1995), pp. 19–33.
30. P. A. Wright, Nitrogen excretion: Three end products, many physiological roles. *J. Exp. Biol.* **198**, 273–281 (1995).
31. M. J. Benton, Z. Zhonghe, P. J. Orr, Z. Fucheng, S. L. Kearns, The remarkable fossils from the early Cretaceous Jehol Biota of China and how they have changed our knowledge of Mesozoic life: Presidential address, delivered 2nd May 2008. *Proc. Geol. Assoc.* **119**, 209–228 (2008).
32. X. Xu, K. Wang, K. Zhang, Q. Ma, L. Xing, C. Sullivan, D. Hu, S. Cheng, S. Wang, A gigantic feathered dinosaur from the Lower Cretaceous of China. *Nature* **484**, 92–95 (2012).
33. P. Godefroit, S. M. Sinitsa, D. Dhouailly, Y. L. Bolotsky, A. V. Sizov, M. E. McNamara, M. J. Benton, P. Spagna, A Jurassic ornithischian dinosaur from Siberia with both feathers and scales. *Science* **345**, 451–455 (2014).
34. Z. Yang, B. Jiang, M. E. McNamara, S. L. Kearns, M. Pittman, T. G. Kaye, P. J. Orr, X. Xu, M. J. Benton, Pterosaur integumentary structures with complex feather-like branching. *Nat. Ecol. Evol.* **3**, 24–30 (2019).
35. P. M. Barrett, D. C. Evans, N. E. Campione, Evolution of dinosaur epidermal structures. *Biol. Lett.* **11**, 20150229 (2015).
36. C. F. Kammerer, S. Nesbitt, J. J. Flynn, L. Ranivoharimanana, A. R. Wyss, A tiny ornithodiran archosaur from the Triassic of Madagascar and the role of miniaturization in dinosaur and pterosaur ancestry. *Proc. Natl. Acad. Sci. U.S.A.* **117**, 17932–17936 (2020).
37. P. R. Bell, N. E. Campione, W. S. Persons IV, P. J. Currie, P. L. Larson, D. H. Tanke, R. T. Bakker, Tyrannosauroid integument reveals conflicting patterns of gigantism and feather evolution. *Biol. Lett.* **13**, 20170092 (2017).
38. M. J. Benton, The origin of endothermy in synapsids and archosaurs and arms races in the Triassic. *Gondw. Res.* **100**, 261–289 (2021).
39. M. G. Baron, D. B. Norman, P. M. Barrett, A new hypothesis of dinosaur relationships and early dinosaur evolution. *Nature* **543**, 501–506 (2017).
40. G. M. Erickson, On dinosaur growth. *Annu. Rev. Earth Planet. Sci.* **42**, 675–697 (2014).
41. N. Klein, C. Foth, R. R. Schoch, Preliminary observations on the bone histology of the Middle Triassic pseudosuchian archosaur *Batrachotomus kupferzellensis* reveal fast growth with laminar fibrolamellar bone tissue. *J. Vertebr. Paleontol.* **37**, e1333121 (2017).
42. A. W. A. Kellner, X. Wang, H. Tischlinger, D. de Almeida Campos, D. W. E. Hone, X. Meng, The soft tissue of *Jeholopterus* (Pterosauria, Anurognathidae, Batrachognathinae) and the structure of the pterosaur wing membrane. *Proc. R. Soc. B* **277**, 321–329 (2010).
43. M. J. Benton, D. Dhouailly, B. Jiang, M. McNamara, The early origin of feathers. *Trends Ecol. Evol.* **34**, 856–869 (2019).
44. M. F. Schaller, J. D. Wright, D. V. Kent, Atmospheric pCO_2 perturbations associated with the Central Atlantic magmatic province. *Science* **331**, 1404–1409 (2011).
45. M. F. Schaller, J. D. Wright, D. V. Kent, P. E. Olsen, Rapid emplacement of the Central Atlantic Magmatic Province as a net sink for CO_2. *Earth Planet. Sci. Lett.* **323-324**, 27–39 (2012).
46. T. K. Knobbe, M. F. Schaller, A tight coupling between atmospheric pCO_2 and sea-surface temperature in the Late Triassic. *Geology* **46**, 43–46 (2018).
47. P. Forster, T. Storelvmo, K. Armour, W. Collins, J.-L. Dufresne, D. Frame, D. J. Lunt, T. Mauritsen, M. D. Palmer, M. Watanabe, M. Wild, H. Zhang, The Earth's Energy Budget, Climate Feedbacks, and Climate Sensitivity in *Climate Change 2021: The Physical Science Basis. Contribution of Working Group I to the Sixth Assessment Report of the Intergovernmental Panel on Climate Change*, V. Masson-Delmotte, P. Zhai, A. Pirani, S. L. Connors, C. Péan, S. Berger, N. Caud, Y. Chen, L. Goldfarb, M. I. Gomis, M. Huang, K. Leitzell, E. Lonnoy, J. B. R. Matthews, T. K. Maycock, T. Waterfield, O. Yelekçi, R. Yu, B. Zhou, Eds. (Cambridge University Press, 2021), chap. 7, pp. 923–1054.
48. M. Hautmann, M. J. Benton, A. Tomašových, Catastrophic ocean acidification at the Triassic-Jurassic boundary. *Neues Jahrb. Geol. Paläontol. Abh.* **249**, 119–127 (2008).
49. C. P. Fox, X. Cui, J. H. Whiteside, K. Grice, Molecular and isotopic evidence reveals the end-Triassic carbon isotope excursion is not from massive exogenous light carbon. *Proc. Natl. Acad. Sci. U.S.A.* **117**, 30171–30178 (2020).
50. J. C. McElwain, Paleobotany and global change: Important lessons for species to biomes from vegetation responses to past global change. *Annu. Rev. Plant Biol.* **69**, 761–787 (2018).
51. H.-D. Sues, P. E. Olsen, Stratigraphic and temporal context and faunal diversity of Permian-Jurassic continental tetrapod assemblages from the Fundy rift basin, eastern Canada. *Atl. Geol.* **51**, 139–205 (2015).
52. M. R. Rampino, S. Self, Volcanic winter and accelerated glaciation following the Toba super-eruption. *Nature* **359**, 50–52 (1992).
53. M. Sigl, M. Winstrup, J. R. McConnell, K. C. Welten, G. Plunkett, F. Ludlow, U. Büntgen, M. Caffee, N. Chellman, D. Dahl-Jensen, H. Fischer, S. Kipfstuhl, C. Kostick, O. J. Maselli, F. Mekhaldi, R. Mulvaney, R. Muscheler, D. R. Pasteris, J. R. Pilcher, M. Salzer, S. Schüpbach, J. P. Steffensen, B. M. Vinther, T. E. Woodruff, Timing and climate forcing of volcanic eruptions for the past 2,500 years. *Nature* **523**, 543–549 (2015).
54. E. G. Dutton, J. R. Christy, Solar radiative forcing at selected locations and evidence for global lower tropospheric cooling following the eruptions of El Chichón and Pinatubo. *Geophys. Res. Lett.* **19**, 2313–2316 (1992).
55. B. van de Schootbrugge, T. M. Quan, S. Lindström, W. Püttmann, C. Heunisch, J. Pross, J. Fiebig, R. Petschick, H.-G. Röhling, S. Richoz, Y. Rosenthal, P. G. Falkowski, Floral changes across the Triassic/Jurassic boundary linked to flood basalt volcanism. *Nat. Geosci.* **2**, 589–594 (2009).

56. K. L. Bacon, C. M. Belcher, M. Haworth, J. C. McElwain, Increased Atmospheric SO_2 detected from changes in leaf physiognomy across the Triassic-Jurassic boundary interval of East Greenland. *PLOS ONE* **8**, e60614 (2013).
57. M. Steinthorsdottir, C. Elliott-Kingston, K. L. Bacon, Cuticle surfaces of fossil plants as a potential proxy for volcanic SO_2 emissions: Observations from the Triassic-Jurassic transition of East Greenland. *Paleobiodivers. Paleoenviron.* **98**, 49–69 (2018).
58. V. Vajda, M. Calner, A. Ahlberg, Palynostratigraphy of dinosaur footprint-bearing deposits from the Triassic-Jurassic boundary interval of Sweden. *GFF* **135**, 120–130 (2013).
59. M. R. Rampino, S. Self, Large igneous provinces and biotic extinctions, in *The Encyclopedia of Volcanoes*, H. Sigurdsson, B. Houghton, S. R. McNutt, H. Rymer, J. Stix, Eds. (Academic Press, 2015), pp. 1049–1058.
60. T. J. Blackburn, P. E. Olsen, S. A. Bowring, N. M. McLean, D. V. Kent, J. Puffer, G. McHone, E. T. Rasbury, M. Et-Touhami, Zircon U-Pb geochronology links the end-Triassic extinction with the Central Atlantic Magmatic Province. *Science* **340**, 941–945 (2013).
61. J. P. Landwehrs, G. Feulner, M. Hofmann, S. Petri, Climatic fluctuations modeled for carbon and sulfur emissions from end-Triassic volcanism. *Earth Planet. Sci. Lett.* **537**, 116174 (2020).
62. J. Brugger, G. Feulner, S. Petri, Baby, it's cold outside: Climate model simulations of the effects of the asteroid impact at the end of the Cretaceous. *Geophys. Res. Lett.* **44**, 419–427 (2017).
63. G. Mantell, ART. XVII. The geological age of reptiles. *Am. J. Sci.* **21**, 359–363 (1832).
64. P. E. Olsen, D. V. Kent, H. D. Sues, C. Koeberl, H. Huber, A. Montanari, E. C. Rainforth, S. J. Fowell, M. J. Szajna, B. W. Hartline, Ascent of dinosaurs linked to an iridium anomaly at the Triassic-Jurassic boundary. *Science* **296**, 1305–1307 (2002).
65. M. A. D. During, J. Smit, D. F. A. E. Voeten, C. Berruyer, P. Tafforeau, S. Sanchez, K. H. W. Stein, S. J. A. Verdegaal-Warmerdam, J. H. J. L. van der Lubbe, The Mesozoic terminated in boreal spring. *Nature* **603**, 91–94 (2022).
66. B. J. Allen, T. L. Stubbs, M. J. Benton, M. N. Puttick, Archosauromorph extinction selectivity during the Triassic-Jurassic mass extinction. *Palaeontology* **62**, 211–224 (2019).
67. R. S. Tykoski, T. B. Rowe, R. A. Ketcham, M. W. Colbert, *Calsoyasuchus valliceps*, a new crocodyliform from the early Jurassic Kayenta formation of Arizona. *J. Vertebr. Paleontol.* **22**, 593–611 (2002).
68. M. G. Baron, *Pisanosaurus mertii* and the Triassic ornithischian crisis: Could phylogeny offer a solution? *Hist. Biol.* **31**, 967–981 (2017).
69. G. F. Barrowclough, J. Cracraft, J. Klicka, R. M. Zink, How many kinds of birds are there and why does it matter? *PLOS ONE* **11**, e0166307 (2016).
70. C. J. Burgin, J. P. Colella, P. L. Kahn, N. S. Upham, How many species of mammals are there? *J. Mammal.* **99**, 1–14 (2018).
71. P. E. Olsen, E. C. Rainforth, in *The Great Rift Valleys of Pangea in Eastern North America: Volume 2: Sedimentology, Stratigraphy, and Paleontology*, P. M. LeTourneau, P. E. Olsen, Eds. (Columbia Univ. Press, 2003), vol. 2, pp. 314–367.
72. L. Tauxe, Inclination flattening and the geocentric axial dipole hypothesis. *Earth Planet. Sci. Lett.* **233**, 247–261 (2005).
73. D. V. Kent, E. Irving, Influence of inclination error in sedimentary rocks on the Triassic and Jurassic apparent pole wander path for North America and implications for Cordilleran tectonics. *J. Geophys. Res.* **115**, B10103 (2010).
74. L. Wu, V. A. Kravchinsky, D. K. Potter, Apparent polar wander paths of the major Chinese blocks since the Late Paleozoic: Toward restoring the amalgamation history of east Eurasia. *Earth Sci. Rev.* **171**, 492–519 (2017).
75. P. Povea, I. Cacho, A. Moreno, M. Menéndez, F. J. Méndez, A new procedure for the lithic fraction characterization in marine sediments from high productivity areas: Optimization of analytical and statistical procedures. *Limnol. Oceanogr-Meth.* **13**, 127–137 (2015).
76. S. J. Nesbitt, The early evolution of archosaurs: Relationships and the origin of major clades. *Bull. Am. Mus. Nat. Hist.* **352**, 1–292 (2011).
77. M. C. Langer, J. Ramezani, Á. A. S. Da Rosa, U-Pb age constraints on dinosaur rise from south Brazil. *Gondw. Res.* **57**, 133–140 (2018).
78. R. T. Müller, M. S. Garcia, Rise of an empire: Analysing the high diversity of the earliest sauropodomorph dinosaurs through distinct hypotheses. *Hist. Biol.* **2019**, 1334–1339 (2019).
79. F. Choulet, Y. Chen, J. P. Cogné, A. Rabillard, B. Wang, W. Lin, M. Faure, D. Cluzel, First Triassic palaeomagnetic constraints from Junggar (NW China) and their implications for the Mesozoic tectonics in Central Asia. *J. Asian Earth Sci.* **78**, 371–394 (2013).
80. T. H. Torsvik, R. van der Voo, U. Preeden, C. Mac Niocaill, B. Steinberger, P. V. Doubrovine, D. J. J. van Hinsbergen, M. Domeier, C. Gaina, E. Tohver, J. G. Meert, P. J. A. McCausland, L. R. M. Cocks, Phanerozoic polar wander, palaeogeography and dynamics. *Earth Sci. Rev.* **114**, 325–368 (2012).
81. D. V. Kent, L. Tauxe, Corrected Late Triassic latitudes for continents adjacent to the North Atlantic. *Science* **307**, 240–244 (2005).
82. A. L. Lottes, D. B. Rowley, Reconstruction of the Laurasian and Gondwanan segments of Permian Pangaea, in *Palaeozoic Palaeogeography and Biogeography*, W. S. McKerrow, C. R. Scotese, Eds. (Geological Society, 1990), pp. 383–395.
83. D. J. van Hinsbergen, L. V. de Groot, S. J. van Schaik, W. Spakman, P. K. Bijl, A. Sluijs, C. G. Langereis, H. Brinkhuis, A paleolatitude calculator for paleoclimate studies. *PLOS ONE* **10**, e0126946 (2015).
84. C. G. Kowalenko, D. Babuin, Inherent factors limiting the use of laser diffraction for determining particle size distributions of soil and related samples. *Geoderma* **193-194**, 22–28 (2013).
85. C. Polakowski, M. Ryżak, A. Bieganowski, A. Sochan, P. Bartmiński, R. Dębicki, W. Stelmach, The reasons for incorrect measurements of the mass fraction ratios of fine and coarse material by laser diffraction. *Soil Sci. Soc. Am. J.* **79**, 30–36 (2015).
86. M. Sperazza, J. N. Moore, M. S. Hendrix, High-resolution particle size analysis of naturally occurring very fine-grained sediment through laser diffractometry. *J. Sediment. Res.* **74**, 736–743 (2004).
87. K. A. Dias, thesis, Stony Brook University, Stony Brook, NY (2014).
88. M. Kottek, J. Grieser, C. Beck, B. Rudolf, F. Rubel, World map of the Köppen-Geiger climate classification updated. *Meteorol. Z.* **15**, 259–263 (2006).
89. M. C. Peel, B. L. Finlayson, T. A. McMahon, Updated world map of the Köppen-Geiger climate classification. *Hydrol. Earth Syst. Sci.* **11**, 1633–1644 (2007).
90. J. Zhang, O. K. Lenz, J. Hornung, P. Wang, M. Ebert, M. Hinderer, Palynology and the Eco-Plant model of peat-forming wetlands of the Upper Triassic Haojiagou Formation in the Junggar Basin, Xinjiang, NW China. *Palaeogeogr. Palaeoclimatol. Palaeoecol.* **556**, 109888 (2020).
91. K. T. Ouyang, H. Ren, Z. H. Xu, F. G. Wang, S. Z. Liu, Q. M. Zhang, M. F. Hu, Y. J. Zhang, Z. J. Liu, Q. F. Guo, Habitat characteristics and population structure of *Dipteris chinensis*, a relict plant in China. *Appl. Ecol. Environ. Res.* **19**, 1939–1951 (2021).
92. B. Bomfleur, H. Kerp, The first record of the dipterid fern leaf *Clathropteris* Brongniart from Antarctica and its relation to *Polyphacelus stormensis* Yao, Taylor et Taylor nov. emend. *Review of Palaeobotany and Palynology* **160**, 143–153 (2010).
93. F. Rivera-Hernandez, D. Y. Sumner, T. J. Mackey, I. Hawes, D. T. Andersen, In a PICL: The sedimentary deposits and facies of perennially ice-covered lakes. *Sedimentology* **66**, 917–939 (2019).
94. R. Gilbert, Rafting in glacimarine environments. *Geol. Soc. Spec. Pub.* **53**, 105–120 (1990).
95. P. E. Olsen, N. McDonald, S. T. Kinney, Lake algal-rafted lithic and biotic debris and the origin of insect Lagerstätten. *Geophys. Res. Abstr.* **20**, 11440–11442 (2018).
96. C. Mendoza-Lera, L. L. Federlein, M. Knie, M. Mutz, The algal lift: Buoyancy-mediated sediment transport. *Water Resour. Res.* **52**, 108–118 (2016).
97. K. O. Emery, Transportation of rocks by driftwood. *J. Sediment. Res.* **25**, 51–57 (1955).
98. P. R. Vogt, M. Parrish, Driftwood dropstones in Middle Miocene Climate Optimum shallow marine strata (Calvert Cliffs, Maryland Coastal Plain): Erratic pebbles no certain proxy for cold climate. *Palaeogeogr. Palaeoclimatol. Palaeoecol.* **323-325**, 100–109 (2012).
99. S. J. Nesbitt, R. J. Butler, M. D. Ezcurra, P. M. Barrett, M. R. Stocker, K. D. Angielczyk, R. M. H. Smith, C. A. Sidor, G. Niedźwiedzki, A. G. Sennikov, A. J. Charig, The earliest bird-line archosaurs and the assembly of the dinosaur body plan. *Nature* **544**, 484–487 (2017).
100. S. J. Nesbitt, C. A. Sidor, K. D. Angielczyk, R. M. H. Smith, L. A. Tsuji, A new archosaur from the Manda beds (Anisian, Middle Triassic) of southern Tanzania and its implications for character state optimizations at Archosauria and Pseudosuchia. *J. Vertebr. Paleontol.* **34**, 1357–1382 (2014).
101. H. N. Bryant, A. P. Russell, The role of phylogenetic analysis in the inference of unpreserved attributes of extinct taxa. *Philos. Trans. R. Soc. Lond. B.* **337**, 405–418 (1992).
102. S. L. Brusatte, M. J. Benton, J. B. Desojo, M. C. Langer, The higher-level phylogeny of Archosauria (Tetrapoda: Diapsida). *J. Syst. Palaeontol.* **8**, 3–47 (2010).
103. N. E. Campione, P. M. Barrett, D. C. Evans, On the ancestry of feathers in Mesozoic dinosaurs, in *The Evolution of Feathers*, C. Foth, W. M. Rauhut, Eds. (Springer, 2020), pp. 213–243.
104. S. Ochiai, K. Kashiwaya, A conceptual model of sedimentation processes for a hydrogeomorphological study in Lake Baikal, in *Long Continental Records from Lake Baikal*, K. Kashiwaya, Ed. (Springer, 2003), pp. 297–312.
105. A. A. Prokopenko, E. B. Karabanov, D. F. Williams, G. K. Khursevich, The stability and the abrupt ending of the last interglaciation in southeastern Siberia. *Quatern. Res.* **58**, 56–59 (2002).
106. Y. Lu, X. Fang, O. Friedrich, C. Song, Characteristic grain-size component–A useful process-related parameter for grain-size analysis of lacustrine clastics? *Quat. Int.* **479**, 90–99 (2018).
107. X. Liu, J. Vandenberghe, Z. An, Y. Li, Z. Jin, J. Dong, Y. Sun, Grain size of Lake Qinghai sediments: Implications for riverine input and Holocene monsoon variability. *Palaeogeogr. Palaeoclimatol. Palaeoecol.* **449**, 41–51 (2016).
108. F. Spindler, R. Werneburg, J. W. Schneider, L. Luthardt, V. Annacker, R. Rößler, First arboreal "pelycosaurs" (Synapsida: Varanopidae) from the early Permian Chemnitz Fossil Lagerstätte, SE Germany, with a review of varanopid phylogeny. *PalZ* **92**, 315–364 (2018).

109. A. G. Sharov, New flying reptiles from the Mesozoic of Kazakhstan and Kirgyzstan. *Trudy Paleontol. Inst.* **130**, 104–113 (1971).
110. W. Bian, J. Hornung, Z. Liu, P. Wang, M. Hinderer, Sedimentary and palaeoenvironmental evolution of the Junggar Basin, Xinjiang, northwest China. *Paleobiodivers. Paleoenviron.* **90**, 175–186 (2010).
111. X. Wang, Z. Zhou, F. Zhang, X. Xu, A nearly completely articulated rhamphorhynchoid pterosaur with exceptionally well-preserved wing membranes and "hairs" from Inner Mongolia, northeast China. *Chin. Sci. Bull.* **47**, 226–230 (2002).
112. X. Xu, X. Zheng, H. You, A new feather type in a nonavian theropod and the early evolution of feathers. *Proc. Natl. Acad. Sci. U.S.A.* **106**, 832–834 (2009).
113. A. Kaiser, thesis, Christian-Albrechts-Universität, Kiel (2002).

Acknowledgments: We are grateful for the assistance of C. Ye (Department of Geosciences, Stony Brook University), K. Joyce and Y. Rosenthal (Department of Earth and Planetary Science, Rutgers University), and H. Yin and X. Yu (Carleton Civil Engineering Lab, Columbia University) on their Mastersizer 2000, Mastersizer 3000, and Mastersizer 2000, respectively. We also thank M. Hill and A. K. Smith (American Museum of Natural History MIF Lab) for SEM imaging and CT data processing and B. Linsley (LDEO) for using Keyence microscope. We thank the LDEO repository and curator N. Anest for access to the core and help with sampling and grain size (including grain size standards), and we thank the OSU repository for providing samples. B.-A. Bhullar produced the CT scan of the Junggar sample and provided helpful suggestions for which he is thanked. This is a contribution to UNESCO-IUGS IGCP project 632 and the CycloAstro Project funded by the Heising-Simons Foundation. **Funding:** This work was supported by the National Natural Science Foundation of China (41730317), the Chinese Academy of Geological Sciences (DD20190009), the Special Basic Program of Ministry of Science and Technology of China (2015FY310100), the Bureau of Geological Survey of China, and the National Committee of Stratigraphy of China (DD20160120-04). The Lamont Climate Center is acknowledged for support to P.O., C.C., and S.K. The LDEO repository is funded by NSF OCE-1259124 and the OSU NSF OCE-1558679. Additional funding was provided by the Heising-Simons Foundation (award no. 2021-2801), the Swedish Research Council (VR grant 2019), and the Knut and Alice Wallenberg (KAW) Foundation. **Author contributions:** Conceptualization: J.S. (lead) and P.O. Methodology: P.O. (lead), C.C., J.S., D.K., J.H.W., H.-D.S., M.S., and V.V. Formal analysis and investigation: C.C., Y.F., S.K. (equal), and J.H.W. Original draft preparation: P.O., J.H.W., D.K., C.C., and J.S. Visualization: P.O. Supervision: J.S. and P.O. (equal). Project administration: J.S. Funding acquisition: J.S. and P.O. **Competing interests:** The authors declare that they have no competing interests. **Data and materials availability:** All data needed to evaluate the conclusions in the paper are present in the paper and/or the Supplementary Materials. Physical subsamples of materials listed with IGSN identifiers in table S1 may be requested from the authors.

Submitted 15 February 2022
Accepted 17 May 2022
Published 1 July 2022
10.1126/sciadv.abo6342

ScienceAdvances

Arctic ice and the ecological rise of the dinosaurs

Paul OlsenJingeng ShaYanan FangClara ChangJessica H. WhitesideSean KinneyHans-Dieter SuesDennis KentMorgan SchallerVivi Vajda

Sci. Adv., 8 (26), eabo6342. • DOI: 10.1126/sciadv.abo6342

Science Advances (ISSN) is published by the American Association for the Advancement of Science. 1200 New York Avenue NW, Washington, DC 20005. The title *Science Advances* is a registered trademark of AAAS.